Synthesis of New Blue Anthracene-based Conjugated Polymers and Their Applications in Polymer Light-Emitting Diodes

Hung-Min Shih, Cheng-Jui Lin, Shin-Rong Tseng, Chih-Hung Lin, Chain-Shu Hsu*

A series of anthracene-based conjugated copolymers containing 9,10-bis(6-bromonaphthalen-2-yl)-2-*tert*-butylanthracene (BNA) and 2,7-diphenyl substituted fluorene (DPPF) moieties are prepared via a palladium-catalyzed Suzuki polymerization. All of the synthesized polymers emit blue light at around 450 nm and show good thermal and color stability. Their electroluminescence spectra remain unchanged at high driving voltage. The double-layer polymer light-emitting diode (PLED) fabricated with ITO/PEDOT:PSS/DPPFBNA3/CsF/Al, produces a maximum brightness of 1 650 $cd \cdot m^{-2}$ and has a luminance efficiency of 0.39 $cd \cdot A^{-1}$. The ITO/PEDOT:PSS/TFB/DPPFBNA3/CsF/Al multilayer PLED, incorporating a TFB layer to facilitate hole transportation, produces a maximum brightness of 5 371 $cd \cdot m^{-2}$ and a luminance efficiency of 1.18 $cd \cdot A^{-1}$.

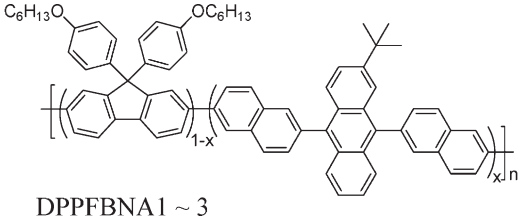

DPPFBNA1 ~ 3

Introduction

Polymer light-emitting diodes (PLEDs) are attracting great interest because of their potential applications in full-color flat panel displays and in solid-state lighting.[1–3] PLED devices fabricated by simple solution processes such as spin coating or inkjet-printing, can provide large-area devices at relatively low cost. Display and lighting applications require the development of efficient and stable, high purity, red, green, and blue light-emitting materials.[4] Of these three elemental colors, the materials for blue light emission remain problematic. Polyfluorenes (PFs) show promise as blue-light-emitting polymers due to their high photoluminescence (PL) quantum efficiency, and good thermal and chemical stability.[5] However, PFs exhibit poor electroluminescence and color stability, due to their intermolecular aggregation of the polymer backbones, and the keto effect.[6,7] Workers report that, device performance improvements are possible by the incorporation of dopants in the polymer chains, due to a charge trapping and energy transfer mechanism.[8] In this study, dopants covalently bonded to the polymer chains facilitate energy transfer between the host polymer and its guest dopants. Diphenylanthracene has high fluorescence quantum yield and good electrochemical properties. Therefore, there is much interest in anthracene derivatives as blue light-emitting materials.[9–14] For example, Zheng et al. synthesized three novel polymers containing the chromophore 9,10-di(2-naphthyl)-anthracene. The polymers showed efficient blue PL both in solution, and in thin films a single layer device produced a luminance efficiency of 0.4 $cd \cdot A^{-1}$. Kwon and co-workers synthesized a new polymer containing alternate diphenylanthracene and carbazole layers in

C.-S. Hsu, H.-M. Shih, C.-J. Lin, S.-R. Tseng
Department of Applied Chemistry, National Chiao Tung University, Hsinchu 30010, Taiwan
Fax: (886) 3 5131523; E-mail: cshsu@mail.nctu.edu.tw
C.-H. Lin
Center for General Education, Chang Gung Institute of Technology, Kwei-Shan, Taoyuan 333, Taiwan

DOI: 10.1002/macp.201000680

the polymer chains, to achieve charge balance. However, the single device had high turn-on voltage of 12.5 V. The researchers also reported a new blue light-emitting polyether, containing diphenylanthracene and benzoxazolylphenyl substitution in the polymer main chain. The incorporation of benzoxazolylphenyl as an electron transport moiety within the polymer chain improved charge transport balance. However, the single layered device emitted blue light at around 15–20 V. Kang et al. introduced a series of blue-light-emitting diphenylanthracene derivatives containing a flexible silylene-spacer in the backbone. The double layered device had a lower turn-on voltage of 4.7 V, a maximum brightness of $\approx$1 000 cd $\cdot$ m^{-2}, and maximum luminance efficiency of the device was about 0.7 cd $\cdot$ A^{-1}. Recently, Kwon and co-workers reported that introducing small molecular chromophore dopants into the polymer prevented the formation of aggregates and improved device performance. At 5.8 V, Kwon and co-workers double layer device had a higher turn-on voltage than the undoped device, and a reduced maximum brightness of 152 cd $\cdot$ m^{-2}, which device performance remained low. Light-emitting devices based on polymers containing an anthracene moiety need to have good performance and stable color emission. However, these reports all showed that blue-light-emitting polymers emit a greenish-blue hue, and the blue emission appears unstable. Furthermore, device performances presented high turn-on voltages and reduced luminance efficiencies. These materials properties need further improvement in order to provide good color stability.

In this work, we prepared a series of anthracene-based conjugated copolymers containing 9,10-bis(6-bromonaphthalen-2-yl)-2-*tert*-butylanthracene (BNA) and 2,7-diphenyl substituted fluorene (DPPF) moieties via a palladium-catalyzed Suzuki polymerization. In DPPF unit, a bulky phenyl-ring at the C-9 position of fluorene units provides a large degree of steric hindrance, and prevents aggregation and intermolecular interactions between polymer chains, resulting in great enhancement of device performance. In order to evaluate the EL performance of the synthesized polymers, we fabricated both double-layered and multilayered devices. The multilayered devices incorporating a poly[(9,9-dioctylfluorenyl-2,7-diyl)-*co*-(4,4′-(*N*-(4-sec-butylphenyl)-diphenylamine)] (TFB) film that acts as an electron-blocking layer, show further improvements in device performance and reduce charge recombination.[15] Such devices were fabricated by using a viscosity liquid buffer layer in order to avoid interfacial mixing with adjacent layers during solution processing. The addition of a super-yellow polymer into the blue emissive polymer can produce white light devices with potential applications in solid-state lighting.[16,17]

Experimental Part

Materials

2,7-Dibromo-9-fluorenone, 2,6-dibromonaphthalene, 2-*t*-butyl-anthaquinone, *n*-butylithium, 4-bromoaniline, 1-iodotolune, tetrakis(triphenylphosphine) palladium, 2-isopropoxy-4,4,5,5-tretramethyl-1,3,2-dioxaborolane, and all other reagents were purchased from Aldrich and used as received tetrahydrofuran, and toluene were distilled over sodium/benzophenone and calcium hydride. Compound **1**, monomer **M1**, monomer **M2**, end-capping reagent **3**, end-capping reagent **4**, and 2,7-bis(4,4,5,5,-tetramethyl-1,3,2-dioxaborolan-2-yl)-9,9-dioctylfluorene (**M4**) was prepared according to reported procedures.[18] The schematic synthesis routes of resulting monomers and polymers are demonstrated in Scheme 1 to 3.

9,10-Bis(6-bromonaphthalen-2-yl)-2-*tert*-butyl-9,10-dihydroanthracene-9,10-diol (2)

A solution of *n*-butyllithium (10.64 mL, 17.1 mmol, 1.6 M solution in hexane) was added slowly to a solution of 2,6-dibromonaphthalene (6.49 g, 22.7 mmol) in anhydrous THF (150 mL) at −78 °C, and the reaction mixture was kept stirring at this temperature for 1 h. Then, a solution of 2-*tert*-butylanthaquinone (3.0 g, 11.4 mmol) in anhydrous THF was added to the mixture. The mixture was allowed to slowly warm up to room temperature and stirred for 12 h. A large amount of water (300 mL) was added to the mixture. The mixture was extracted with ethyl acetate. The combined organic layers were dried over anhydrous $MgSO_4$ and the solvent was removed under reduced pressure. The crude product was purified by column chromatography (silica gel, hexane/ethyl acetate: 4:1 was used as the eluent) to yield 5.94 g (77%) white solid. ^{1}H NMR (300 MHz, $CDCl_3$): δ(ppm) = 1.32 (s, 9H, C$\underline{H}_3$), 2.93 (s, 1H, –O$\underline{H}$), 2.98 (s, 1H, –O$\underline{H}$), 6.98 (s, 1 aromatic proton), 7.02 (d, J = 5.1 Hz, 3H, aromatic protons), 7.23 (dd, J = 1.5 Hz, J = 8.7 Hz, 2 aromatic protons), 7.29 (d, J = 2.1 Hz, 1 aromatic proton), 7.31 (d, J = 1.8 Hz, 1H, aromatic proton), 7.35 (d, J = 8.7 Hz, 2 aromatic protons), 7.41–7.48 (m, 2 aromatic protons), 7.66 (s, 2 aromatic protons), 7.71 (d, J = 8.1 Hz, 2 aromatic protons), 7.75–7.83 (m, 3 aromatic protons). ^{13}C NMR (75 MHz, $CDCl_3$): δ(ppm) = 31.3, 34.8, 75.1, 75.4, 120.1, 123.6, 125.4, 126.1, 126.3, 126.4, 126.4, 126.5, 126.5, 126.7, 126.8, 128.2, 128.9, 129.4, 130.5, 133.0, 138.1, 140.3, 141.1, 141.2, 141.6, 141.7, 151.4. MS (FAB-MS): m/z = 678 (M^+).

9,10-Bis(6-bromonaphthalen-2-yl)-2-tert-butylanthracene (BNA-Br2)

Compound **2** (7.08 g, 10.4 mmol), potassium iodide (6.24 g, 37.6 mmol), and sodium hypophosphite hydrate (7.52 g, 70.9 mmol) were dissolved in acetic acid (100 mL) and the reaction mixture was stirred at 110 °C for 2 h. After cooling to room temperature, the yellow precipitate was filtered, then washed with water, and dried to yield 6.05 g (90%) light yellow solid. ^{1}H NMR (300 MHz, $CDCl_3$): δ(ppm) = 1.22 (s, 9H, C$\underline{H}_3$), 7.28–7.33 (m, 2 aromatic protons), 7.44 (dd, J = 2.1 Hz, J = 9.3 Hz, 1 aromatic proton), 7.62–7.70 (m, 8 aromatic protons), 7.78–7.83 (m, 2 aromatic protons), 7.97–8.03 (m, 4 aromatic protons), 8.20–8.21 (m, 2 aromatic protons). ^{13}C NMR (75 MHz, $CDCl_3$): δ(ppm) = 30.7, 34.9, 120.2, 121, 124.8, 124.9, 125.1, 126.1, 126.8, 127.1, 128.6, 129.8,

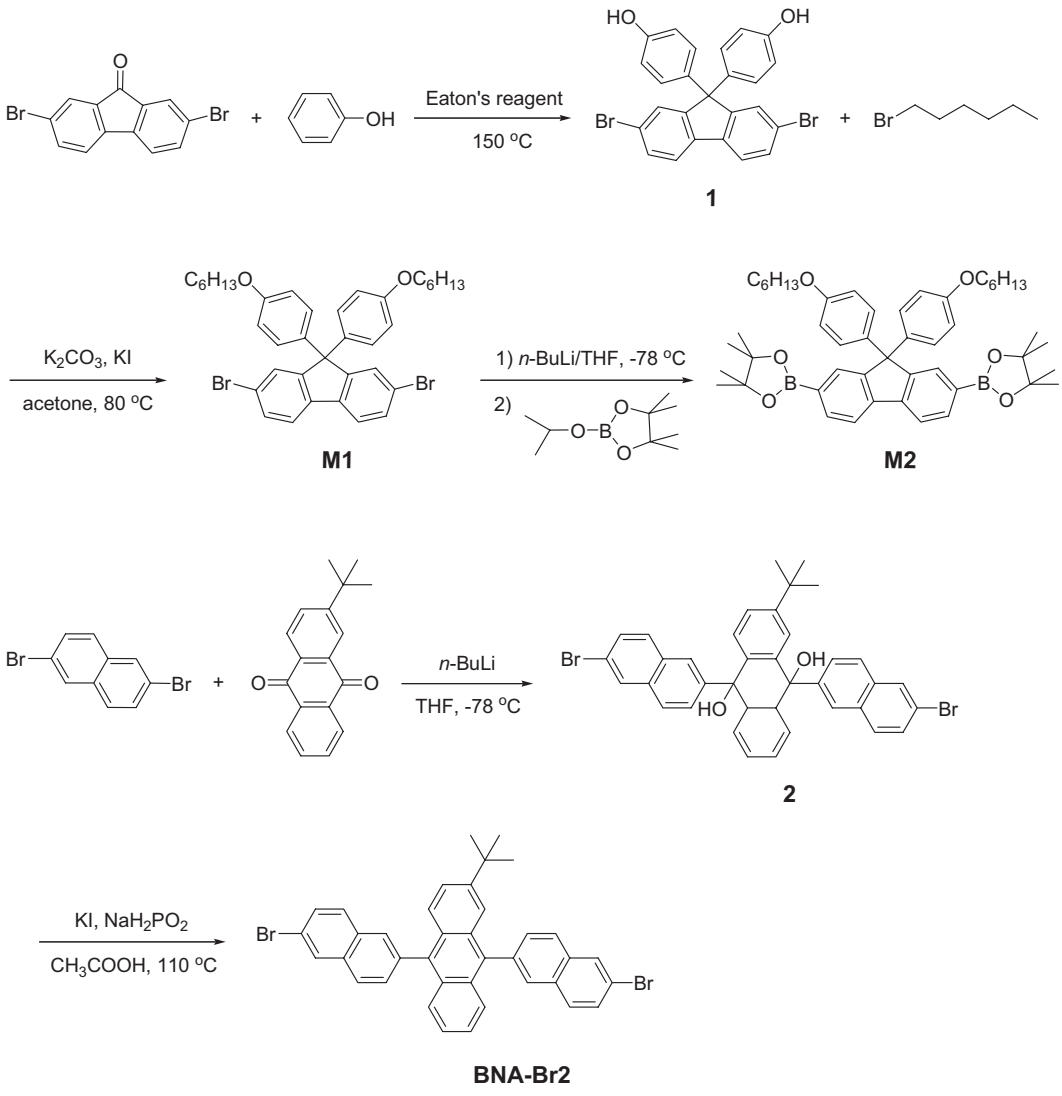

Scheme 1. Synthesis of monomers **M1**, **M2**, and **BNA-Br2**.

129.9, 130.2, 130.6, 131.8, 133.8, 136.2, 136.4, 137.2, 147.7. MS (FAB-MS): $m/z = 644$ (M^+). Anal. Calcd. for $C_{38}H_{30}Br_2$: C 70.60, H 4.68; Found: C 70.47, H 4.78.

Preparation of Poly[9,9′-dioctylfluorene-*co*-9,10-bis(6-naphthalen-2-yl)-2-tert-butylanthracene] (PFBNA)

A mixture of **BNA-Br2** (300 mg, 0.46 mmol), **M4** (299 mg, 0.46 mmol), $Pd(PPh_3)_4$ (0.01 g, 0.0093 mmol), aliquat 336 (0.06 g, 0.14 mmol), and aqueous K_2CO_3 (2 M, 2 mL) in degassed toluene (15 mL) was stirred at 85 °C for 5 d under a nitrogen atmosphere. The end-capping reagent **3** (0.10 g, 0.28 mmol) was added to the solution and stirred at 85 °C for 12 h and then end-capping reagent **4** (0.10 g, 0.25 mmol) was added to the solution and stirred at 85 °C for another 12 h. After cooling to room temperature, the reaction mixture was poured into methanol (200 mL) and the crude polymer precipitated. The polymer was purified by several re-precipitation steps from THF solution into methanol and was further purified by soxhlet extraction with acetone for 72 h. The final polymer was dried under vacuum to yield 0.23 g (58%) yellowish green solid.

Preparation of Poly[9,9′-bis(4-hexyloxyphenyl)-fluorene-*co*-9,10-bis(6-naphthalen-2-yl)-2-tert-butylanthracene] (DPPFBNA 1-3)

Three PFs DPPFBNA1-DPPFBNA3 were synthesized via palladium-catalyzed Suzuki polymerization. The synthesis of DPPFBNA2 was given as an example. A mixture of **BNA-Br2** (125 mg, 0.19 mmol), **M1** (132 mg, 0.19 mmol), **M2** (300 mg, 0.38 mmol), $Pd(PPh_3)_4$ (0.0090 g, 0.0078 mmol), aliquat 336 (0.07 g, 0.17 mmol), and aqueous K_2CO_3 (2 M, 2 mL) in degassed toluene (10 mL) was stirred at 85 °C for 5 d under a nitrogen atmosphere. The end-capping reagent **3** (0.1 g, 0.28 mmol) was added to the solution and stirred at 85 °C for 12 h and then end-capping reagent **4** (0.1 g, 0.25 mmol) was added to the solution and stirred at 85 °C for another 12 h. After cooling to room temperature, the reaction mixture was poured into

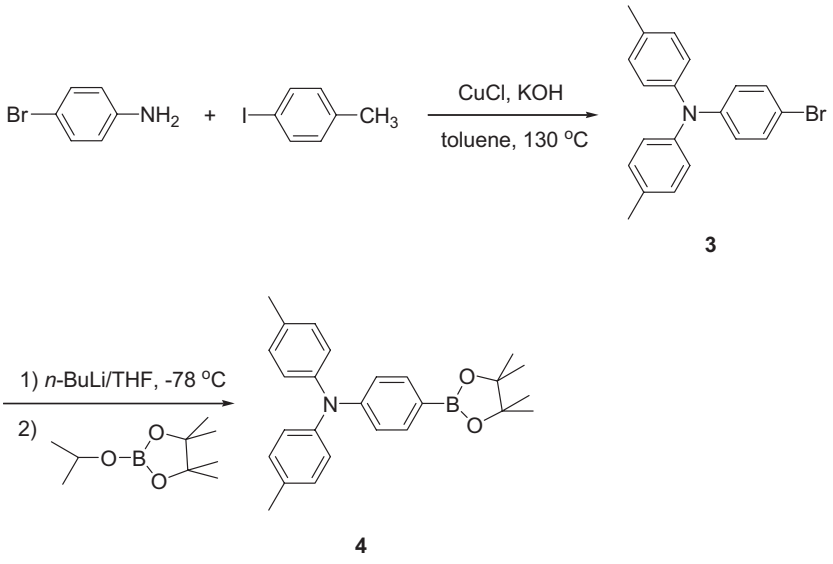

Scheme 2. Synthesis of end-capping reagents **3** and **4**.

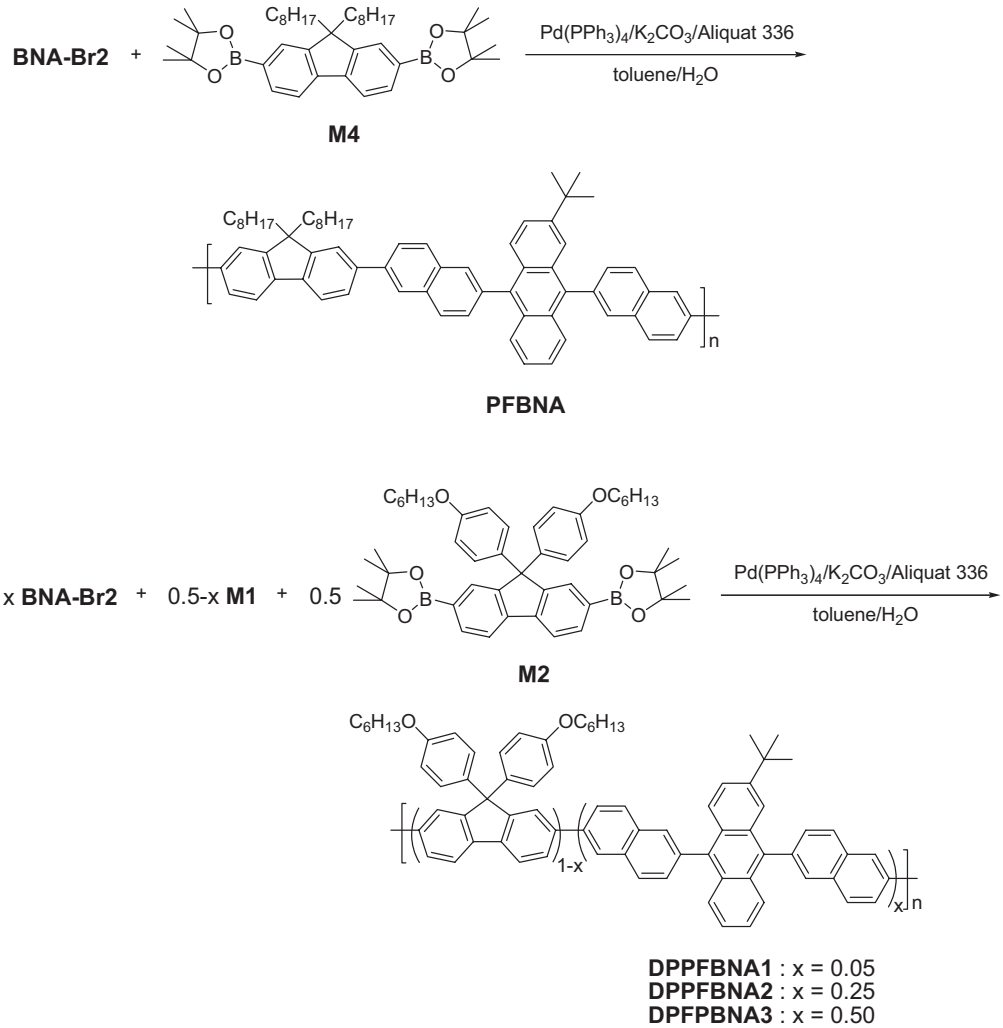

Scheme 3. Synthesis of PFBNA and DPPFBNA1-DPPFBNA3 PFs.

methanol (200 mL) and the crude polymer was precipitated. The polymer was purified by several reprecipitation steps from THF solution into methanol and was further purified by soxhlet extraction with acetone for 72 h. The final polymer was dried under vacuum to yield 0.27 g (70%) dark green solid.

Characterization

^{1}H and ^{13}C NMR spectra were recorded on a Varian-300 MHz spectrometer. Mass spectra were obtained using a JEOL JMS-HX 110 mass spectrometer. Gel permeation chromatography (GPC) was measured using a Viscotek GPC system equipped with a Viscotek T50A differential viscometer, and Viscotek LR125 laser referactometer. Three 10 μm American Polymer columns were connected in series in order of decreasing the pore size (10^5, 10^4, and 10^3 Å), polystyrene standards were used for calibration, and THF was used as the eluent. Differential scanning calorimetry (DSC) was performed on a TA Q Series DSC unit operated at a heating and cooling rate of 10 °C · min^{-1}, respectively. Thermogravimetric analysis (TGA) was carried out using a Perkin Elmer Pyris 7 instrument. UV–Vis spectra were measured using an HP 8453 spectrophotometer. PL spectra were obtained using an ARC SpectraPro-150 luminescence spectrometer. Cyclic voltammetry (CV) experiments were performed using an Autolab ADC 164 electrochemical analyzer operated at a scanning rate of 50 mV ·s^{-1}; the supporting electrolyte was 0.1 M tetra-*n*-butylammonium tetrafluoroborate (*n*-Bu_4NBF_4) which was dissolved in CH_2Cl_2. The potentials were measured against an Ag/AgCl reference electrode using ferrocene/ferrocenium (Fc/Fc^+) as the internal standard.

Device Fabrication and Measurements

The patterned ITO glass substrates were ultrasonically cleaned with detergent, deionized water, acetone, and isopropyl alcohol. The PEDOT:PSS was spin-coated on the cleaned and UV-ozone treated ITO substrates. The PEDOT:PSS layer was baked at 200 °C for 15 min in air to remove residual water and then moved into a glove box under nitrogen. TFB ($\overline{M}_w$ = 50 000–10 000 g · mol^{-1}, purchased from American Dye Sources) as a hole transport layer was dissolved in toluene solution (10 mg · mL^{-1}) and was spin-coated on the PEDOT:PSS layer and then heated at 180 °C at 30 min under nitrogen. For multilayer device fabrication, all copolymers dissolved in toluene solution (1.5 wt.-%) were spin-coated on the TFB layer by using a buffer liquid method[15] and then baked at 80 °C for 30 min under vacuum. CsF (2 nm)/Al (100 nm) were thermal deposited as cathodes. The current–voltage–luminance characteristics were measured using an optical power meter PR-650 and a digital source meter Keithley 2400. The EL spectra were measured using a Photo Research PR-650 spectrophotometer under ambient condition after encapsulation.

Results and Discussion

Table 1 summarizes the polymerization results and thermal properties of the obtained copolymers. The number average molecular weights ($\overline{M}_n$) range from 2.3×10^4 to 6.3×10^4 g · mol^{-1}, as determined by GPC, and polydispersities (PDI) were around 1.40. Both PFBNA and DPPFBNA2 have glass transition temperatures at around 100 °C, while the DPPFBNA1 glass transition temperature is less, at 86 °C. This lower glass transition temperature is due to its lower molecular weight and reduced BNA content. DPPFBNA3 showed no glass transition temperature (T_g) since it contained 50% rigid BNA. All copolymers showed good thermal stability and their thermal decomposition temperatures (T_d) ranged from 400 to 460 °C.

Optical Properties

Figure 1 presents UV–Vis absorption, and PL spectra of all copolymers, both in solution, and in thin films, while Table 2 summarizes the spectral data. The PL quantum yields of the copolymers in solution are about 61–88%, and in thin films is about 14–25%. This reduction is a result of copolymer aggregation in the thin films, and subsequent self-quenching, which reduces the observed PL. This aggregation is evidence of enhanced intermolecular and intramolecular interactions between conjugated backbone chains. The UV–Vis spectra in Figure 1a shows that in solution, increasing BNA content across the series of DPPFBNA copolymers causes a blue shift in the spectrum. The shoulders at 378 and 396 nm are the result of absorption by BNA's anthracene group.[19] According to literature reports, the main fluorene absorption occurs at 390 nm, and anthracene's absorption peaks are at 359, 377, 396 nm.[20] Thus, the observed blue shift results from the apparent increase in absorption by the anthracene-group, seen for increasing BNA content in the polymer, especially at the shorter wavelength of 349 nm. In Figure 1a, the PL plot

Table 1. Monomer feed ratios, polymer average molecular weights and thermal properties.

Polymer	Feed ratio	$\overline{M}_w$	$\overline{M}_n$	PDI	T_d	T_g
	mol-%	$\times 10^4$	$\times 10^4$	$\overline{M}_w/\overline{M}_n$	°C	°C
PFBNA	**BNA-Br2** (50)/**M4** (50)	8.81	6.30	1.40	458	98
DPPFBNA1	**BNA-Br2** (5)/**M1** (45)/**M2** (50)	3.18	2.25	1.41	404	86
DPPFBNA2	**BNA-Br2** (25)/**M1** (25)/**M2** (50)	6.39	4.54	1.41	400	103
DPPFBNA3	**BNA-Br2** (50)/**M2** (50)	6.70	4.84	1.38	426	–

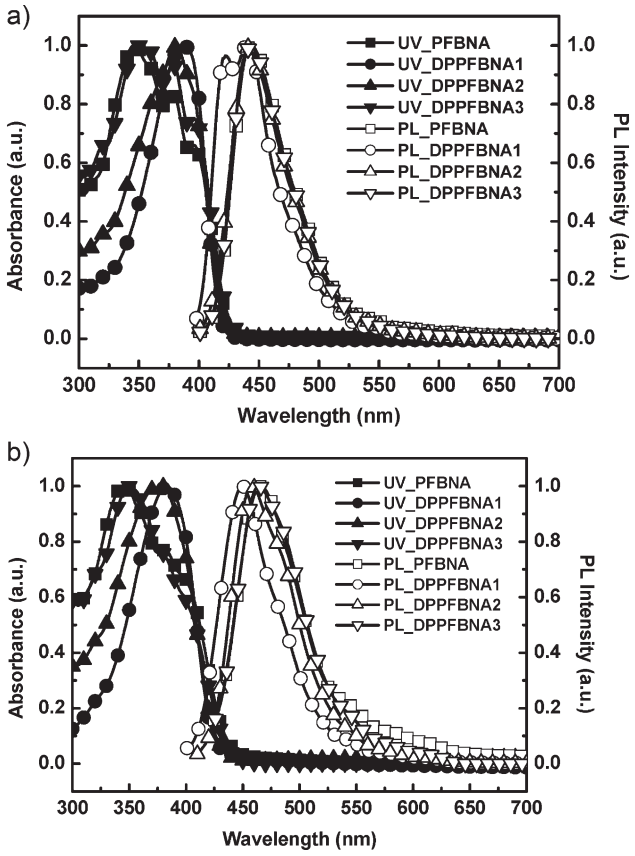

Figure 1. The UV–Vis and PL spectra of the copolymers (a) in solution and (b) in thin film.

shows a shoulder at 422 nm for those polymers containing only 5% BNA, which results from emission by the fluorene repeating unit.[21–23] With increasing BNA content, the interaction between fluorene structures in the polymer decreases. The observation indicates that energy transfer from the polymer backbone to the anthracene moiety is more efficient due to a lowering in energy of the lowest unoccupied molecular orbital (LUMO) in the anthracene. Figure 1b shows that the thin film UV–Vis spectra in which the absorption peak exhibits an ≈3 nm blue shift in comparison with the solution spectra. The PL emission spectra in thin films are determined to be red shifted compared to the solution spectra. In 5% BNA polymer, the PL spectra are red-shifted about 10 nm compared to the solution spectrum. In addition, the appearance of the red shift increased to about 20 nm when the BNA content in the polymer was 25 or 50%. This observation suggests that aggregation of polymer in thin films causes the addition of conjugated sections of the polymer. The emission maximum shifted to longer wavelength with increase of coplanar BNA content compared with the substituted fluorene containing phenyl ring. We studied the thermal stability of all copolymers, and measured their PL spectra as thin films. The thin films of all copolymers were spin-coated onto quartz glass from a chloroform solution (15 mg · mL^{-1}), moved into an oven, and annealed at 150 °C for 2 h in air. Figure 2 shows the PL spectra of PFBNA and DPPFBNA3 thin films after thermal annealing. The figure shows that none of the copolymers produced a green emission between 530 and 550 nm. All copolymers emitted blue light, demonstrating that the fluorene side-chain phenyl rings prevents the formation of fluorenone and promotes thermal stability of polymers. The result showed that the phenyl ring in the fluorene side-chains produced enhanced color stability by comparison with alkyl chains at the C-9 position of fluorene.[24] To our surprise, the PFBNA polymer containing the fluorene units with alkyl side chains shows also no green emission after long time annelling at high temperature. This result could be due to two reasons: first, fluorenone defects do not formed, or second, the BNA units play as a competing energy trap in this copolymer, and therefore the fluorenone unit is silent.[25]

Electrochemical Properties

We investigated the oxidation behavior of all copolymers, and estimated and their highest occupied molecular orbital (HOMO) energy levels by CV. All copolymer samples were dissolved in dichloromethane solution during the electrochemical processes, and monitored in a standard three-electrode electrochemical cell using ferrocene/ferrocenium ion (Fc/Fc^+) as the internal standard. The electrolyte was

Table 2. Optical properties of PFBNA and DPPFBNA1 ≈ DPPFBNA3.

Polymer	$\lambda_{max}^{Abs,THF}$	$\lambda_{max}^{Abs,film}$	$\lambda_{max}^{PL,THF}$	$\lambda_{max}^{PL,film}$	Φ_{PL}^{THF}	Φ_{PL}^{film}
	nm	nm	nm	nm	nm	nm
PFBNA	347, 378[a], 396[a]	345, 381[a]	444	466	61	14
DPPFBNA1	386	383	442, 422[a]	450	88	25
DPPFBNA2	381	378	442	458	69	24
DPPFBNA3	349, 378[a], 396[a]	350	445	464	67	21

[a]Shoulder peak.

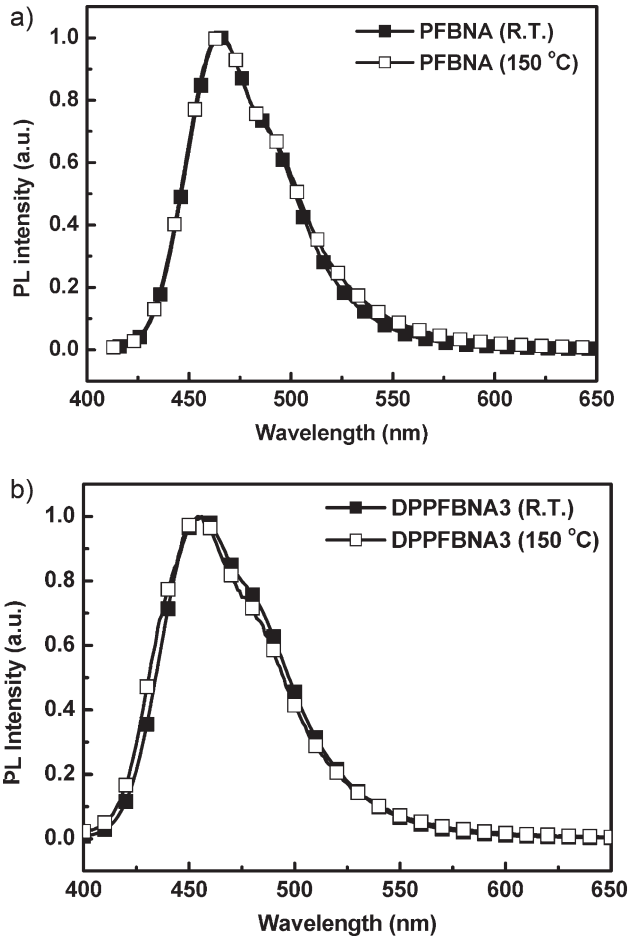

Figure 2. The PL spectra of the thin films, recorded after annealing at 150 °C for 2 h in air (a) PFBNA and (b) DPPFBNA3.

0.1 M n-Bu_4NBF_4 dissolved in CH_2Cl_2 solution and the scanning rate was 50 $mV \cdot s^{-1}$. Table 3 compares the electrochemical properties of all copolymers with an alkyl-substituted PF (PFBNA). The synthesized copolymers have very similar electrochemical properties to the literature reported PF, with $E_{ox} = 1.4$ V and IP = 5.8 V.[26] PFBNA and DPPFBNA3 were alternating copolymers, while DPPFBNA1 and DPPFBNA2 were random copolymers, which possessed various amount of BNA monomer units. PFBNA and DPPFBNA3 share the same HOMO and LUMO energy levels. The DPPFBNA2 HOMO energy level is lowest at −5.83 V. We consider that the lowest HOMO energy level might be due to the more BNA content in the polymer backbones. Figure 3 summarizes these data as an energy level diagram for the fabricated devices.

Table 3. Polymer electrochemical properties.

Polymer	E_g [a)]	E_{ox} [b)]	HOMO [c)]	LUMO [d)]
	eV	eV	eV	eV
PFBNA	2.82	−1.5	−5.9	−3.08
DPPFBNA1	2.91	−1.51	−5.91	−3
DPPFBNA2	2.9	−1.43	−5.83	−2.93
DPPFBNA3	2.83	−1.49	−5.89	−3.06

[a)]The edge of UV spectrum in thin film state; [b)]the onset of oxidation potential; [c)]the equation HOMO = −4.4 + $E_{ox,\ onset}$; [d)]the equation LUMO = E_g + HOMO.

Electroluminescence Properties

We fabricated two different device designs, and studied the EL characteristics of all copolymers. The double layer devices were fabricated with the configuration of ITO/PEDOT:PSS (50 nm)/EML (70–80 nm)/CsF (2 nm)/Al (100 nm). The multilayer devices were fabricated with the configuration of ITO/PEDOT:PSS (50 nm)/TFB (20 nm)/EML (50–60 nm)/CsF (2 nm)/Al (100 nm). The TFB layer served as both hole transporting and electron blocking functions. We fabricated the multilayer devices by using a buffer layer in order to avoid interfacial mixing between adjacent layers. Table 4 and 5 summarize performance

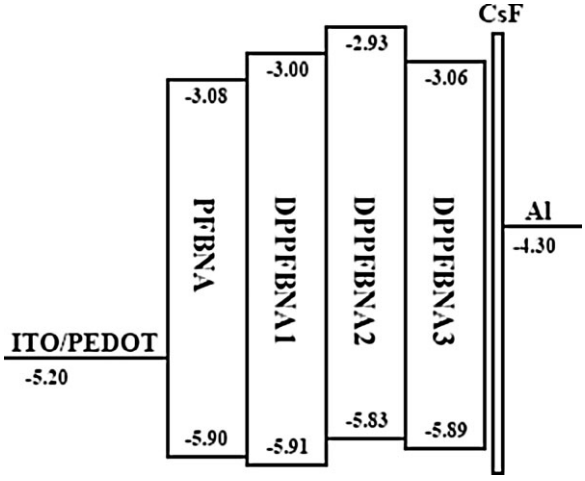

Figure 3. Energy level diagram for all copolymers used in the devices.

Table 4. Polymer performances in the double layer devices.

Polymer	V_{on} [a)]	B_{max}	LE_{max}	EL [b)]	CIE 1931 [b)]
	V	$cd \cdot m^{-2}$	$cd \cdot A^{-2}$	nm	(x, y)
PFBNA	10.9	403	0.11	484	(0.25, 0.27)
DPPFBNA1	5.0	425	0.08	480	(0.19, 0.26)
DPPFBNA2	7.0	741	0.18	472	(0.18, 0.24)
DPPFBNA3	7.8	1650	0.39	484	(0.20, 0.28)

Double layer device: ITO/PEDOT/Polymer/CsF/Al. [a)]Recorded at 1 $cd \cdot m^{-2}$; [b)]recorded at 11 V.

Table 5. Polymer performances in the multilayer devices.

Polymer	V_{on} [a]	B_{max}	LE_{max}	EL [b]	CIE 1931 [b]
	V	$cd \cdot m^{-2}$	$cd \cdot A^{-1}$	nm	(x, y)
TFB/PFBNA	4.5	2 777	0.59	452	(0.16, 0.14)
TFB/DPPFBNA1	4.6	3 760	0.5	444	(0.17, 0.14)
TFB/DPPFBNA2	4.5	5 261	0.95	452	(0.16, 0.15)
TFB/DPPFBNA3	4.5	5 371	1.18	456	(0.16, 0.19)

Multilayer device: ITO/PEDOT/TFB/Polymer/CsF/Al. [a]Recorded at 1 $cd \cdot m^{-2}$; [b]recorded at 8 V.

results for the devices. The inset in Figure 5 indicates that all copolymers produce good blue emissions. For comparison purpose, we synthesized PFBNA which containing alkyl side-chains in the fluorene units. Its device performance showed a maximum luminance efficiency of 0.11 $cd \cdot A^{-1}$ with a green–blue emission. DPPFBNA3 yields a maximum brightness of 1 650 $cd \cdot m^{-2}$ and has a maximum luminance efficiency of 0.39 $cd \cdot A^{-1}$ (Figure 4 and 5). Its luminance efficiency is threefold greater than that of PFBNA. The luminance output, and luminance efficiency, of the DPPFBNA series polymers increased with increasing BNA content within the polymer. Incorporation BNA units in the polymer enhanced device efficiency by host–guest energy transfer. The current efficiency improved by incorporation of a bulky phenyl-ring at the C-9 position of fluorene introduced a large steric hindrance and prevented polymer aggregation, and resulting in an improvement in current efficiency. Hence, the performance results of series DPPFBNA polymers with increasing BNA in polymer backbones were higher than those of PFBNA. To improve efficiency further, we balanced charge injection and transport mechanisms by fabricating a multilayer device

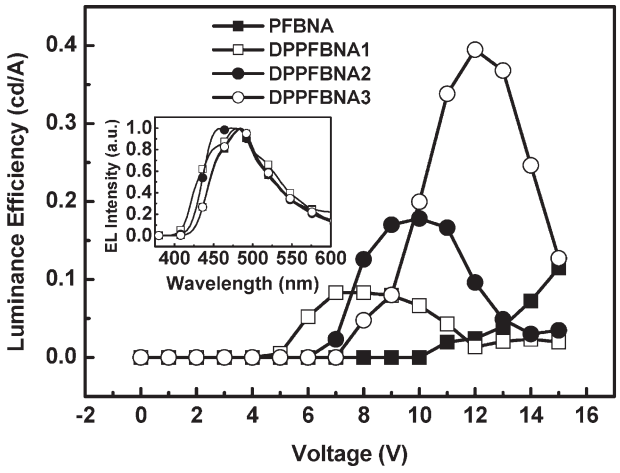

Figure 5. Luminance efficiency plots versus voltage for double layer devices. The inset shows the EL spectrum at 11 V.

containing a TFB layer to afford a hole-transportation. As shown in the inset of Figure 7, all these copolymers exhibited blue green emissions and the color emissions were all stable. DPPFBNA3 also had a maximum brightness of 5 371 $cd \cdot m^{-2}$ and maximum luminance efficiency of 1.18 $cd \cdot A^{-1}$ (Figure 6 and 7). The luminance efficiency was twofold higher than that of PFBNA. The performance of multilayer devices was better than that of double layer devices, and the multilayer device turn-on voltage decreased with the inclusion of the hole-transporting layer. Since the TFB layer was very thin (25 nm), both PL spectra of DPPFBNA 3 and TFB/DPPFBNA3 in thin film states were the same. Both spectra were also similar with the EL spectra of multilayer devices (TFB/DPPFBNA3) in Figure 7. It meant that the TFB layer had no contribution to the EL intensity and served as a hole-transporting layer. The device performance was improved by adding a thin TFB layer which facilitated charge injection and transport.

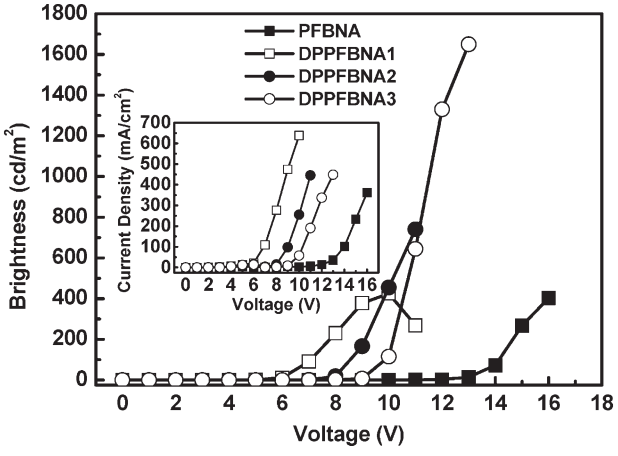

Figure 4. Brightness plots versus voltage for double layer devices. The inset shows current density plots versus voltage.

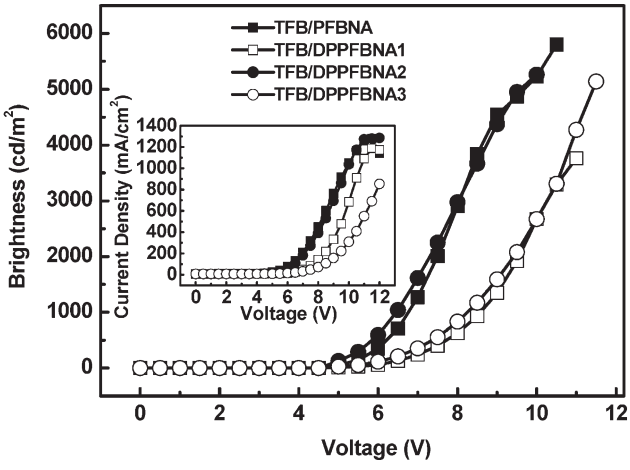

Figure 6. Brightness plots versus voltage for multilayer devices. The inset shows the current density plots versus voltage.

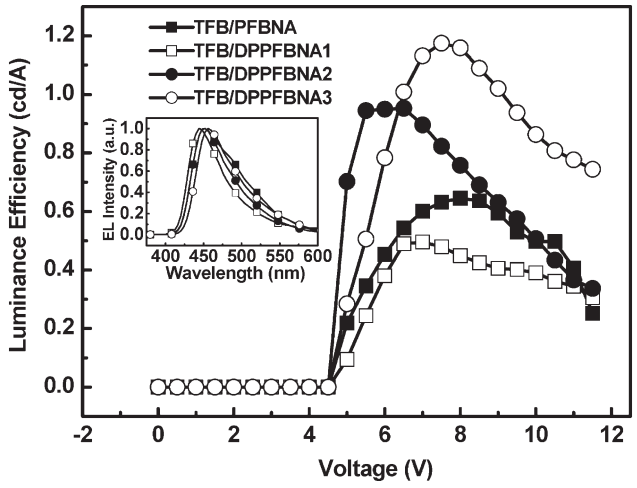

Figure 7. Luminance efficiency plots versus voltage for multilayer devices. The inset shows the EL spectrum at 8 V.

Conclusion

We synthesized a series of blue-emitting copolymers containing anthracene functionality in the polymer chain. All copolymers showed good thermal and color stability, exhibiting blue light emission. Incorporation of BNA into the polymer reduced intermolecular interactions, and produced a green fluorescence due to the keto effect. Increasing the amount of BNA substitution in the polymer backbone enhances performance efficiency. The double layered PLED, fabricated as ITO/PEDOT:PSS/DPPFBNA3/CsF/Al, produced the maximum brightness of 1 650 $cd \cdot m^{-2}$, and had a luminance efficiency of 0.39 $cd \cdot A^{-1}$. Moreover, the multilayer PLED fabricated with the configuration of ITO/PEDOT:PSS/TFB/DPPFBNA3/CsF/Al using the TFB as a hole transporting layer, displayed the maximum brightness of 5 371 $cd \cdot m^{-2}$ and current efficiency of 1.18 $cd \cdot A^{-1}$. By adding the TFB layer, the device performance showed an improvement because of more facile the charge injection and transport.

Acknowledgements: The authors are grateful for financial support from *National Science Council of Taiwan, R.O.C.*

Received: October 30, 2010; Revised: December 21, 2010; Published online: February 25, 2011; DOI: 10.1002/macp.201000680

Keywords: anthracene; blue polymer light-emitting diodes; buffer layer; conjugated polymers; films; fluorene

[1] J. H. Burroughes, D. D. C. Bradley, A. R. Brown, R. N. Marks, K. Mackay, R. H. Friend, P. L. Burn, A. B. Holmes, *Nature* **1990**, *347*, 539.
[2] S. Tasch, E. J. E. List, O. Ekström, W. Graupner, G. Leising, P. Schlichting, U. Rohr, Y. Geerts, U. Scherf, K. Müllen, *Appl. Phys. Lett.* **1997**, *71*, 2883.
[3] [3a] J. Kido, M. Kimura, K. Nagai, *Science* **1995**, *267*, 1332; [3b] S. H. Yang, C. S. Hsu, *J. Polym. Sci., Polym. Chem.* **2009**, *47*, 2713.
[4] C. D. Müler, A. Falcou, N. Reckefuss, M. Rojahn, V. Wiederhirn, P. Rudati, H. Frohne, O. Nuyken, H. Becker, K. Meerholz, *Nature* **2003**, *421*, 829.
[5] U. Scherf, E. J. W. List, *Adv. Mater.* **2002**, *14*, 477.
[6] E. J. W. List, R. Guentner, P. S. Freitas, U. Scherf, *Adv. Mater.* **2002**, *14*, 374.
[7] M. Sims, D. D. C. Bradley, M. Ariu, M. Koeberg, A. Astimakis, M. Grell, *Adv. Funct. Mater.* **2004**, *14*, 765.
[8] [8a] F. Huang, L. T. Hou, H. L. Shen, J. X. Jiang, F. Wang, H. Y. Zhen, Y. Cao, *J. Mater. Chem.* **2005**, *15*, 2499; [8b] F. Huang, L. T. Hou, H. L. Shen, R. Q. Yang, Q. Hou, Y. Cao, *J. Polym. Sci., Part A: Polym. Chem.* **2006**, *44*, 2521; [8c] F. Huang, Y. Zhang, M. S. Liu, Y. J. Cheng, K. Y. Jen, *Adv. Funct. Mater.* **2007**, *17*, 3808.
[9] R. Benzman, L. R. Faulkner, *J. Am. Chem. Soc.* **1972**, *94*, 6317.
[10] S. Zheng, J. Shi, *Chem. Mater.* **2001**, *13*, 4405.
[11] Y. H. Kim, K. M. Bark, S. K. Kwon, *Bull. Korean Chem. Soc.* **2001**, *22*, 975.
[12] Y. H. Kim, S. K. Kwon, *J. Appl. Polym. Sci.* **2006**, *100*, 2151.
[13] T. Lee, K. H. Song, I. Jung, Y. Kang, S. H. Lee, S. O. Kang, J. Ko, *J. Organomet. Chem.* **2006**, *691*, 1887.
[14] S. O. Kim, H. C. Jung, M. J. Lee, C. Jun, Y. H. Kim, S. K. Kwon, *J. Polym. Sci., Part A: Polym. Chem.* **2009**, *47*, 5908.
[15] [15a] S. R. Tseng, S. C. Lin, H. F. Meng, H. H. Liao, C. H. Yeh, H. C. Lai, S. F. Horng, C. S. Hsu, *Appl. Phys. Lett.* **2006**, *88*, 163501; [15b] S. R. Tseng, S. Y. Li, H. F. Meng, Y. H. Yu, C. M. Yang, H. H. Liao, S. F. Horng, C. S. Hsu, *J. Appl. Phys.* **2007**, *101*, 084510.
[16] J. Huang, G. Li, E. Wu, Q. Xu, Y. Yang, *Adv. Mater.* **2006**, *18*, 114.
[17] R. H. Lee, H. F. Hsu, *J. Appl. Polym. Sci.* **2007**, *106*, 2863.
[18] [18a] P. H. Wang, M. S. Ho, S. H. Yang, K. B. Chen, C. S. Hsu, *J. Polym. Sci., Part A: Polym. Chem.* **2010**, *48*, 516; [18b] H. Zengin, G. Zengin, C. M. Topping, D. W. Smith, Jr., *J. Polym. Sci., Part A: Polym. Chem.* **2007**, *45*, 1860; [18c] M. Ranger, D. Rondeau, M. Leclerc, *Macromolecules* **1997**, *30*, 7686.
[19] J. Sun, J. G. Cheng, W. Q. Zhu, S. J. Ren, H. L. Zhong, D. L. Zeng, E. J. Xu, Y. C. Liu, Q. Fang, *J. Polym. Sci., A. Polym. Chem.* **2008**, *46*, 5616.
[20] G. Klarner, M. H. Davey, W. D. Chen, J. C. Scott, R. D. Miller, *Adv. Mater.* **1998**, *10*, 993.
[21] J. H. Ahn, C. Wang, I. F. Perepichka, M. R. Bryce, M. C. Petty, *J. Mater. Chem.* **2007**, *17*, 2996.
[22] D. H. Hwang, J. D. Lee, M. J. Park, *J. Nonlinear Opt. Phys. Mater.* **2004**, *13*, 637.
[23] D. H. Hwang, M. J. Park, J. H. Lee, *Mater. Sci. Eng., C* **2004**, *24*, 201.
[24] [24a] K. B. Chen, H. Y. Chen, S. H. Yang, C. S. Hsu, *J. Polym. Res.* **2006**, *13*, 237; [24b] C. H. Yang, C. J. Bhongale, C. H. Chou, S. H. Yang, C. N. Lo, T. M. Chen, C. S. Hsu, *Polymer* **2007**, *48*, 116; [24c] S. R. Tseng, S. Y. Li, H. F. Meng, Y. H. Yu, C. M. Yang, H. H. Liao, S. F. Horng, C. S. Hsu, *Org. Electron.* **2008**, *9*, 310.
[25] [25a] I. I. Perepiochka, I. I. Perepiochka, M. R. Bryce, L. Pålsson, *Chem. Commun.* **2005**, 3397; [25b] J. Lui, J. Zou, W. Yang, H. Wu, C. Li, B. Zhang, J. Peng, Y. Cao, *Chem. Mater.* **2008**, *20*, 4499; [25c] S. L. McFarlane, D. G. Piercey, L. S. Coumont, R. T. Tucker, M. D. Fleischauer, M. J. Brett, J. G. C. Veinot, *Macromolecules* **2009**, *42*, 591.
[26] S. Janietz, D. D. C. Bradley, M. Grell, C. Giebeler, M. Inbasekaran, E. P. Woo, *Appl. Phys. Lett.* **1998**, *73*, 2453.